Data in Brief 40 (2022) 107696

Contents lists available at ScienceDirect

Data in Brief

journal homepage: www.elsevier.com/locate/dib

Data Article

Dataset for the synthesis, characterisation and application of cobalt and nitrogen co-doped TiO_2 *anatase* nanoparticles on triclosan photodegradation using visible LED light

Olga Ferreira[a,b], Olinda C. Monteiro[c,d], Ana M. Botelho do Rego[e,f], Ana M. Ferraria[e,f], Mary Batista[c], Elisabete R. Silva[a,b,d,*]

[a] *BioISI- Biosystems and Integrative Sciences Institute, Faculdade de Ciências, Universidade de Lisboa, Campo Grande, Lisboa 1749-016, Portugal*
[b] *CERENA- Centro de Recursos Naturais e Ambientais, Instituto Superior Técnico, Universidade de Lisboa, Avenida Rovisco Pais 1, Lisboa 1049-001, Portugal*
[c] *Centro de Química Estrutural, Faculdade de Ciências, Universidade de Lisboa, Campo Grande, Lisboa 1749-016, Portugal*
[d] *Departamento de Química e Bioquímica, Faculdade de Ciências, Universidade de Lisboa, Campo Grande, Lisboa 1749-016, Portugal*
[e] *BSIRG, iBB, DEQ, Instituto Superior Técnico, Universidade de Lisboa, Av. Rovisco Pais, Lisboa 1049-001, Portugal*
[f] *Associate Laboratory i4HB- Institute for Health and Bioeconomy at Instituto Superior Técnico, Universidade de Lisboa, Av. Rovisco Pais, Lisboa 1049-001, Portugal*

ARTICLE INFO

Article history:
Received 17 November 2021
Revised 3 December 2021
Accepted 7 December 2021
Available online 10 December 2021

ABSTRACT

The growing threat of emerging waterborne contaminants is a global concern, fuelled in part by the ineffectiveness of current remediation strategies. One of the most prominent remediation strategies is catalytic photodegradation, particularly with TiO_2 nanoparticles (NPs), but its full utilization is hampered by using only UV radiation, which is scarce in sunlight. To fully benefit from the sunlight abundance, several efforts are focused on the tailoring of TiO_2 to make it more active in visible (Vis) light. However, this target is yet to be

DOI of original article: 10.1016/j.jece.2021.106735
* Corresponding author at: BioISI- Biosystems & Integrative Sciences Institute, Faculdade de Ciências, Universidade de Lisboa, Campo Grande, Lisboa 1749-016, Portugal
E-mail address: ersilva@fc.ul.pt (E.R. Silva).

https://doi.org/10.1016/j.dib.2021.107696
2352-3409/© 2021 The Authors. Published by Elsevier Inc. This is an open access article under the CC BY-NC-ND license (http://creativecommons.org/licenses/by-nc-nd/4.0/)

Keywords:
Titanium dioxide
co-doping
Cobalt
Nitrogen
Visible-light active
Photocatalysis
Triclosan degradation
Monochromatic LED lights

met, sought for new developments. In a recent research paper entitled **"Visible light-driven photodegradation of triclosan and antimicrobial activity against *Legionella pneumophila* with cobalt and nitrogen co-doped TiO_2 *anatase* nanoparticles" [1],** we investigated the co-doping potential of cobalt and nitrogen in TiO_2 NPs for water decontamination, focusing on its application for the degradation of triclosan (TCS) under Vis LED light irradiation. Herein, the synthesis methodology for the preparation of doped TiO_2 with nitrogen is described in detail, along with complementary data on the characterisation of all previously synthesised photocatalysts in the form of specific surface area determination (B.E.T. method) based on the obtained physisorption isotherms, X-ray photoelectron spectroscopy (XPS), and the automatic determination of bandgap energy through the diffuse reflectance spectra (DRS) analysis by using the GapExtractor© software. This dataset article also includes optimised photocatalytic reaction conditions, specifically conducted under monochromatic LED light irradiation. The employed LED irradiation conditions can support photocatalytic research in the field, since LED systems are costless and have a long-life span compared to most conventional UV-Vis systems. In addition, raw UV-Vis spectra and high-performance liquid chromatography (HPLC) chromatograms for monitoring the TCS degradation reaction are also included, as are powder X-ray diffractograms (XRD) of recycled doped-TiO_2 photocatalysts, confirming the renewable efficiency of the synthesised photocatalysts to pursue green chemistry principles.

© 2021 The Authors. Published by Elsevier Inc.
This is an open access article under the CC BY-NC-ND license (http://creativecommons.org/licenses/by-nc-nd/4.0/)

Specifications Table

Subject	Chemical Engineering: Catalysis
Specific subject area	Inorganic chemistry, physical and chemical characterisation, photocatalysis, advanced oxidation processes
Type of data	Figures, Images and Tables.
How the data were acquired	**B.E.T.** physisorption isotherms were acquired on a Quantachrome NOVA 2200e. **XPS** were acquired in a dual anode KRATOS XSAM800 spectrometer supported by the Vision 2 for Windows, Version 2.2.9 software, and using a non-monochromatic AlKα X-ray source (1486.7 eV), produced with a current of 10 mA and an anode voltage of 12 kV, operating at Fixed Analyzer Transmission (FAT) mode, with a pass energy of 20 eV. The powder samples were prior mounted on the sample holder through a double-side tape and further analysed using 90° and 30° take-off angles (relative to the surface plane) in an ultrahigh vacuum chamber ($\sim 10^{-7}$ Pa) at room temperature. **DRS** were acquired in a UV-Vis spectrometer Shimadzu UV-2600PC equipped with an ISR 2600 plus integrating sphere, in the wavelength range of 200-800 nm. Prior to the analysis a baseline correction was performed with the barium sulphate ($BaSO_4$) optical reference. **UV-Vis** spectra were acquired in a Shimadzu UV-1900 spectrophotometer. For data acquisition a band width of 1 nm, medium response, and a scanning speed of 400 nm/min were used. Prior to the analysis a baseline correction with the photocatalytic reaction solvent was performed.

(*continued on next page*)

	HPLC chromatograms were acquired in a VWR-Hitachi Elite LaChrom equipped with a Column Oven L-2300, a LiChroCART 100 RP-18 (5 µm, 100 Å, 250 × 4 mm, Merck) column with reversed phase properties, a Diode Array Detector L-2455 and an automatic injector L-2200. Raw data were acquired using the software EZChrom Elite in a wavelength range of 200 nm to 500 nm with a 1 nm wavelength step, and working under an isocratic mode for 15 min at a flow rate of 0.8 mL/min with 70% acetonitrile and 30% water.
	XRD spectra were acquired in a Philips Analytical, PW 3050/60 with the automatic data acquisition X'Pert Data Collector v.2.0b software and employing a CuKα radiation (λ = 0.15406 nm) working at 40 kV/30 mA. The diffraction patterns were acquired in a 2θ ranging from 20° to 60° with a 0.017° step size and acquisition time of 40.0 s/step. Prior to data acquisition, the powder samples were mounted on a silicon amorphous sample holder.
	LED-photoreaction system: The photocatalytic activity was evaluated by the photodegradation of 10 mL of pure TCS solutions (10 ppm) or those containing dispersed TiO_2-based powder nanoparticles (1 g/L). The solutions and dispersions were placed in 40 mL borosilicate vials and further exposed to monochromatic irradiation (λ = 450 nm) provided by a blue LED lamp (3.4 W at 100% light intensity), for periods between time zero (60 min under dark conditions) and a maximum of 60 min, under a continuous magnetic stirring (900 rpm) and a controlled set temperature (SP= 35 °C) regulated by a fan and a coupled J-type thermocouple (simplex, IEC60584, ΔT= - 40-350 °C). TCS solutions and post-reaction TCS solutions were further analysed by UV-Vis and HPLC.
Data format	Raw and analysed.
Description of data collection	**Prior to analysis:** **B.E.T.**- Powder samples were pre-treated for 2.5 h at 150°C under vacuum (10^{-2} Pa). **DRS** - Powders samples were compressed into $BaSO_4$. **HPLC**- Reaction solutions were filtered using a syringe-filter (0.22 µm). **Corrective factors:** **XPS**- Electric charge accumulation was corrected using carbon peak (set at 285 eV) as reference. **XRD**- Data was normalised to the maximum (101) plane reflection.
Data source location	Faculdade de Ciências, Universidade de Lisboa, Campo Grande 1749-016, Lisboa, Portugal (38.7565° N, 9.1554° W); Instituto Superior Técnico, Universidade de Lisboa, Avenida Rovisco Pais, Lisboa, Portugal (38.7368° N, 9.1387° W).
Data accessibility	Data can be found as an excel supplementary file.
Related research article	O. Ferreira, O.C. Monteiro, A.M. Botelho do Rego, A.M. Ferraria, M. Batista, R. Santos, S. Monteiro, M. Freire, E.R. Silva, *Visible light-driven photodegradation of triclosan and antimicrobial activity against Legionella pneumophila with cobalt and nitrogen co-doped TiO_2 anatase nanoparticles*, J. Environ. Chem. Eng. 9(6) (2021) 106735. https://doi.org/10.1016/j.jece.2021.106735

Value of the Data

- This article provides important data from various analyses (i.e., B.E.T., XPS and DRS), which is highlighted by the automatic determination of bandgap energy using the GapExtractor© software, of novel Co and N co-doping TiO_2-based nanocatalysts which can be useful for characterising analogous nanomaterials and application of such nanomaterials for catalyst designing.
- Based on the data, activated reactions with the co-doping catalysts for the triclosan degradation, monitored by UV-Vis and HPLC, can be considered useful by researchers working in the fields of water treatment and purification for triclosan-containing effluents studies, allowing them to address the poor removal of triclosan in aqueous effluents.

- The data provided on LED light reaction conditions using a more sustainable system can also be usefully considered by academic and industrial researchers in the field of water treatment for upgrading and scaling-up studies in advanced oxidation processes involving triclosan or other emerging pollutants in aqueous effluents.

1. Data Description

The data in this article pertains to the synthesis and characterisation of TiO_2-based nanoparticles (NPs), including undoped TiO_2, TiO_2 doped with nitrogen (TiO_2-N), TiO_2 doped with cobalt (Co-TiO_2) and TiO_2 co-doped with cobalt and nitrogen (Co-TiO_2-N), as well as the photocatalytic ability in degrading triclosan, a common antimicrobial agent and prominent aquatic pollutant, under visible LED light irradiation, assessed to the best nanophotocatalysts described in detail in *Visible light-driven photodegradation of triclosan and antimicrobial activity against Legionella pneumophila with cobalt and nitrogen co-doped TiO_2 anatase nanoparticles* [1].

The B.E.T. adsorption/desorption isotherm data of the various synthesized TiO_2-based NPs are provided as a supplementary file (B.E.T. worksheet), and the resulting isotherm profiles are shown in Fig. 1, along with the calculated apparent surface areas ($A_{B.E.T.}$) from these data.

XPS was used to determine the elemental composition and oxidation states of the different elements on the surface of the synthesised NPs. XPS wide scan spectra of the TiO_2-based NPs are shown in Fig. 2 and raw data which originate them are provided in the supplementary file (XPS worksheet). The detailed spectral fitting parameters for C 1s, O 1s, Ti 2p, Co 2p and N 1s chemical states are summarized elsewhere [1].

The bandgap (*Eg*) of the synthesised NPs were determined using an automated algorithmic method [2] based on the diffuse reflectance spectroscopy data (Fig. 3). The raw data used in the algorithm are provided in the supplementary file (DRS worksheet). This method identifies linear segments in Tauc plots (Fig. 4), further used to estimate the *Eg* value (Table 1). The *Eg* data values for undoped TiO_2 NPs and for nitrogen doped (TiO_2-N) are remarkably similar, with **TiO_2-N** having a slightly higher *Eg* **(3.07 ± 0.08 eV)** than undoped **TiO_2 (3.05 ± 0.10 eV)** NPs. On the other hand, the *Eg* of cobalt doped TiO_2-based NPs showed a significant reduction, with *Eg* values of **2.88 ± 0.10 eV** for **Co-TiO_2-N** and **2.82 ± 0.19 eV** for **Co-TiO_2**.

The photocatalytic activity of the produced doped TiO_2 NPs was further analysed, except for theTiO_2-N NPs since their *Eg* was very close to that of the undoped TiO_2 NPs, making these N-doped TiO_2 NPs less interesting for photocatalytic purposes under Vis light.

The UV-Vis raw data of the post-reaction TCS solutions after photodegradation under Vis (450 nm) light exposure conditions are provided in the supplementary file (UV-Vis-TCS Photocatalysis worksheet), and the originated spectra profiles are shown in Fig. 5.

HPLC analyses of those post-reaction TCS solutions, as well as TCS solutions under dark conditions (adsorption conditions), were also performed to quantify the TCS in solution. A series of TCS aqueous standard solutions were previously prepared and analysed for calibration purposes. The chromatograms obtained at representative TCS concentrations of 0.01, 0.05, 0.1, 1 and 5 mg/L, as well as 10, 20, and 50 mg/L are shown in Fig. 6 (a) and (d) and magnified to the area of interest (retention time = 6.4-8 min) in Fig. 6 (b) and (e). The obtained data for calibration of each concentration range are shown in Fig. 6 (c) and (f). The raw and the analysed data are also provided in the supplementary file (HPLC_calibration data worksheet).

The HPLC chromatograms of the TCS solutions after photodegradation under Vis (450 nm) LED light irradiation are shown in Fig. 7, along with the magnification of the area of interest (retention time = 6.5-8 min) in Fig. 8. The raw and analysed data are provided in the supplementary file (HPLC_Post reaction solutions worksheet).

Fig. 9 (a) shows the adsorption and photodegradation profiles obtained overtime of TCS aqueous solutions in the presence and absence (photolysis) of the synthesised nanocatalysts and originated from acquired raw data. According to these data, no significant TCS was adsorbed on the tested NPs under dark conditions, whereas light irradiation significantly decreased the TCS quantity (degradation yields increased) in the presence of co-doped TiO_2 (Co-TiO_2-N) NPs,

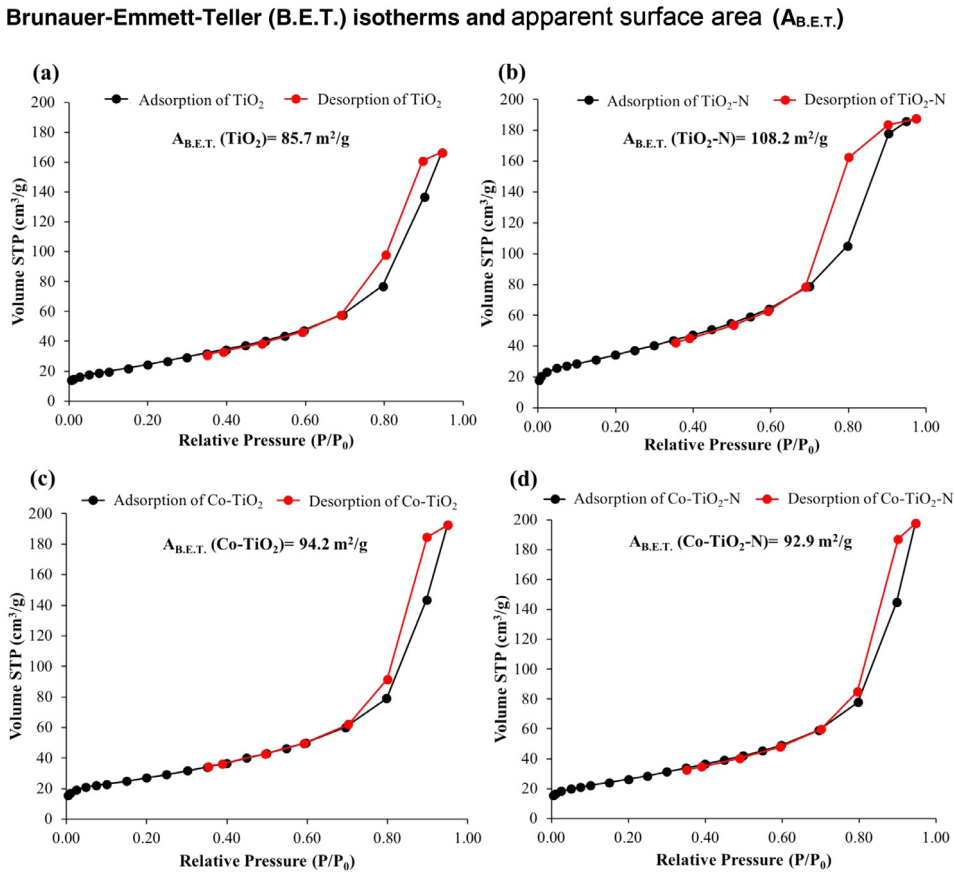

Fig. 1. B.E.T. adsorption/desorption isotherms of (a) TiO_2, (b) TiO_2 doped with nitrogen (TiO_2-N), (c) TiO_2 doped with cobalt (Co-TiO_2) and (d) co-doped with cobalt and nitrogen (Co-TiO_2-N), including the respective apparent surface areas ($A_{B.E.T.}$).

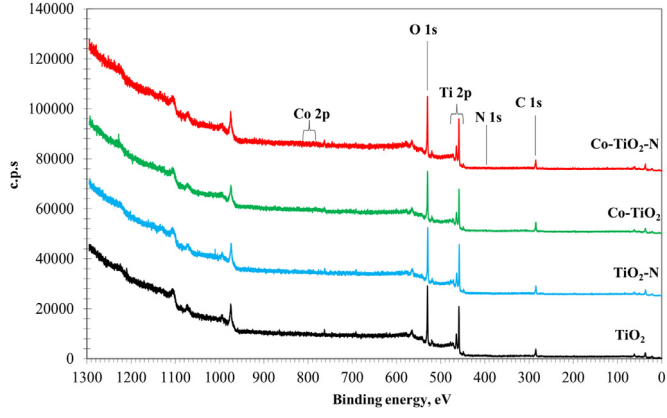

Fig. 2. XPS wide scan spectra of TiO_2, TiO_2 doped with nitrogen (TiO_2-N), TiO_2 doped with cobalt (Co-TiO_2) and co-doped with cobalt and nitrogen (Co-TiO_2-N).

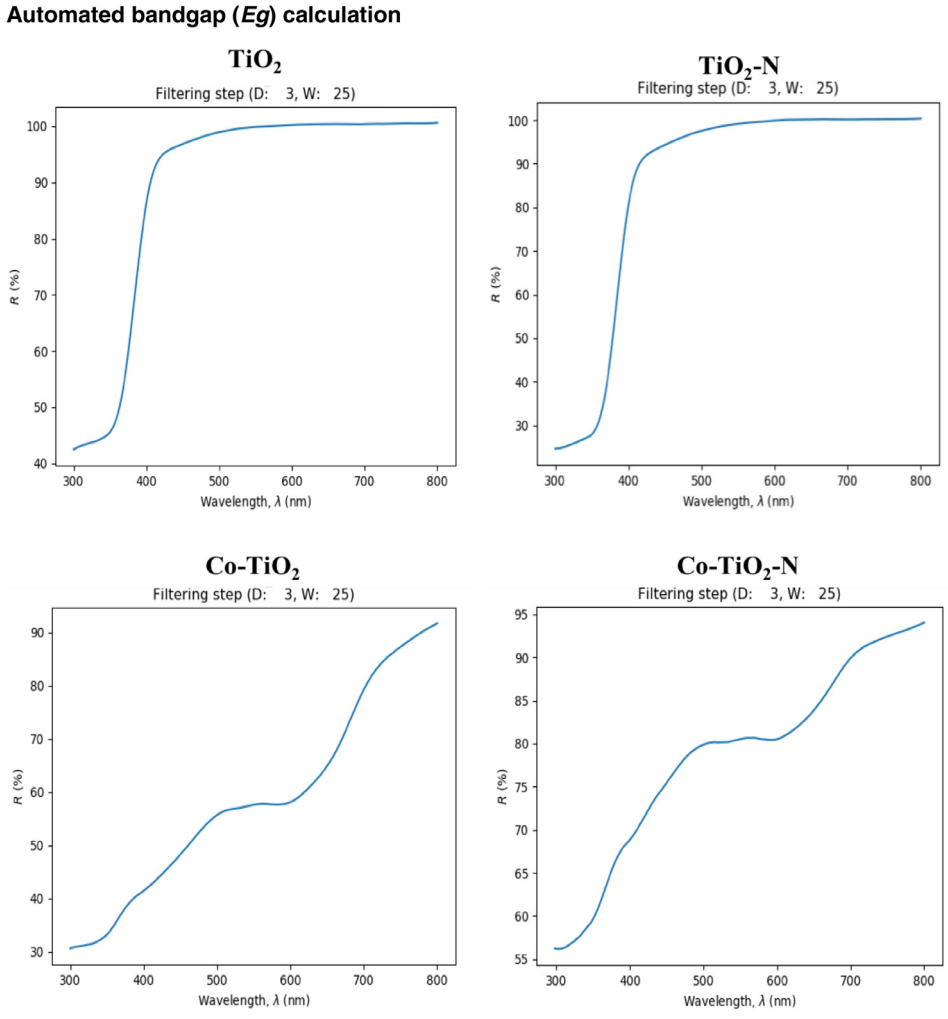

Fig. 3. Diffuse reflectance profiles for the TiO_2, nitrogen doped TiO_2 (TiO_2-N), cobalt doped TiO_2 (Co-TiO_2), and cobalt and nitrogen co-doped TiO_2 (Co-TiO_2-N) nanocatalysts, originated by the Gap extractor© v1.0.

with almost maximum TCS degradation after a 20-min exposure time. The photocatalytic data presented in this data in brief was obtained through replicated analysis, which statically supplements the previously reported results [1]. The kinetic data in Fig. 9 (b) shows that the TCS photolysis and that **TiO_2, Co-TiO_2 and Co-TiO_2-N** had k_{app} values of **0.0075 ± 0.0002 min^{-1}, 0.0516 ± 0.003 min^{-1}, 0.2023 ± 0.012 min^{-1}** and **0.2552 ± 0.010 min^{-1}**, respectively. The k_{app} value of the **Co-TiO_2-N** is the highest under the tested conditions (slightly acidic media, pH = 6, and 450 nm LED light irradiation).

All original data used to obtain Fig. 9, resulting from the degradation and kinetic fitting data described above, are provided in a supplementary Excel file in the Photocatalytic and kinetic data worksheet.

XRD was used to validate the structural stability of the catalysts after photodegradation, and no significant changes were observed between the original XRD spectra and after the fourth successive run (Fig. 10) despite some observed cobalt leaching from the NPs [1]. XRD raw data is provided in supplementary file (XRD worksheet).

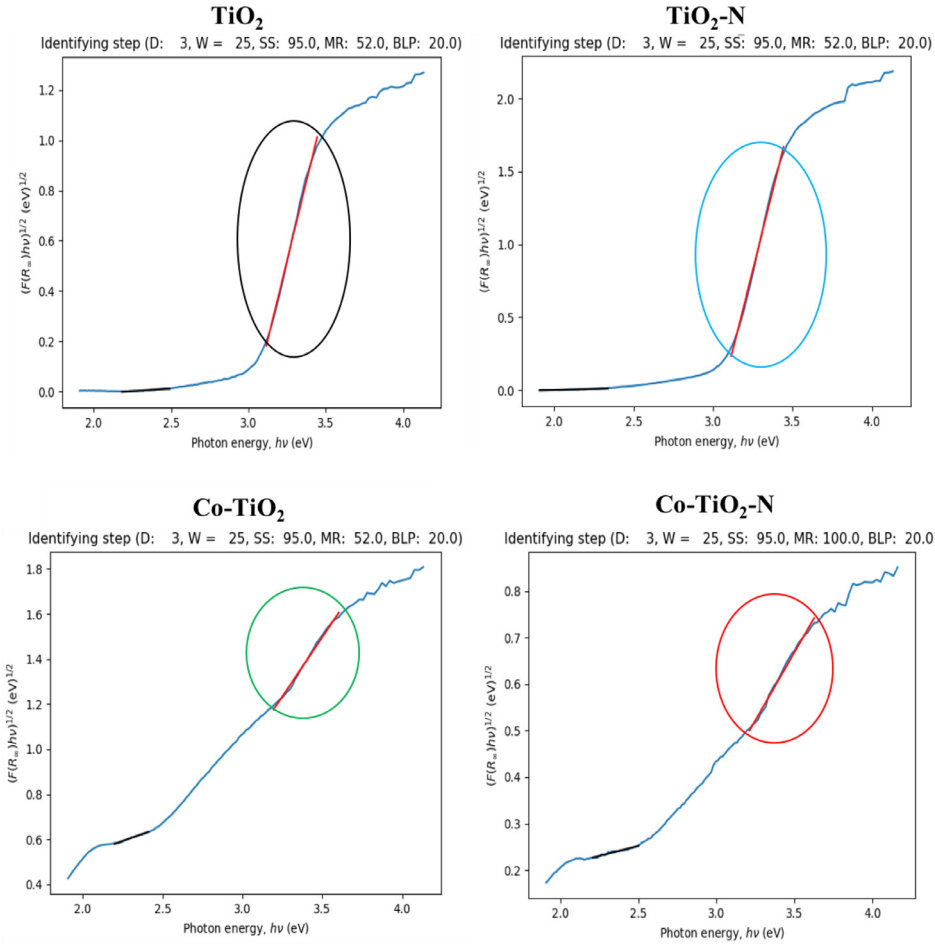

Fig. 4. Tauc plot (f_{KM} vs hυ) straight-line segments regions obtained from Gap extractor© v1.0 for the TiO_2, nitrogen doped TiO_2 (TiO_2-N), cobalt doped TiO_2 (Co-TiO_2), and cobalt and nitrogen co-doped TiO_2 (Co-TiO_2-N) nanocatalysts.

2. Experimental Design, Materials and Methods

2.1. TiO_2-based nanoparticles synthesis

By refining a previously published hydrothermal methodology [4,5], TiO_2-based nanoparticles (NPs) doped with nitrogen (TiO_2-N) were prepared. The synthesis conditions of nitrogen doped TiO_2 nanoparticles add to and complement our previously reported work [1].

Synthesis of nitrogen doped TiO_2 NPs: A titanium source, titanium (III) chloride solution (20 wt% $TiCl_3$ in 2M HCl, Acros), was diluted in a 1:2 ratio of 2M HCl (from a standard hydrochloric acid 37% HCl, AR grade, Sigma-Aldrich). A solution of ammonia (NH_4OH) (4M) (25% NH_3, Panreac) was added dropwise to 75 mL of the diluted solution while vigorously stirring to induce the precipitation of a white solid. After this mixing step, the stirring was ceased, and the suspension was left at room temperature overnight (about 15 h). Afterwards, the suspension was subjected to filtration and the collected precipitate was thoroughly washed with deionized water and dried at room temperature. The dried precipitate, the TiO_2 precursor 1, was redispersed in

Table 1
Report obtained from Gap extractor© v1.0 [2] with the computed bandgap energies (*Eg*), linear segments and Tauc plot (f_{KM} vs hυ) straight-line segments regions for the TiO_2, TiO_2 doped with nitrogen (TiO_2-N), TiO_2 doped with cobalt (Co-TiO_2), and TiO_2 co-doped with cobalt and nitrogen (Co-TiO_2-N) nanocatalysts. Modified from [1].

	Attributes	
Attribute ID	TiO_2	TiO_2-N
(a)	*Eg*= 3.05 ± 0.10 eV	*Eg*= 3.07 ± 0.08 eV
	Linear segments (y= mx+b)	Linear segments (y= mx+b)
(b)	Base line: 1.6060 ≤ hν ≤ 2.3571 eV	Base line: 1.5498 ≤ hν ≤ 2.0325 eV
(c)	m= -3.8943 × 10^{-3} ± 4.2207 × 10^{-4}	m= -3.1214 × 10^{-3} ± 5.0393 × 10^{-4}
(d)	b= 1.0597 × 10^{-2} ± 8.2145 × 10^{-4}	b= 7.1771 × 10^{-3} ± 8.9456 × 10^{-4}
(e)	R-square= 0.411	R-square= 0.290
(f)	Tauc: 3.1629 eV ≤ hν ≤ 3.4250 eV	Tauc: 3.1468 eV ≤ hν ≤ 3.4250 eV
(g)	m= 2.6096 ± 3.9241 × 10^{-2}	m= 4.5281 ± 5.4896 × 10^{-2}
(h)	b= -7.9617 ± 1.2917 × 10^{-1}	b= -1.3902 × 10^{1} ± 1.8024 × 10^{-1}
(i)	R-square= 0.997	R-square= 0.998
	Co-TiO_2	**Co-TiO_2-N**
(a)	*Eg*= 2.82 ± 0.19 eV	*Eg*= 2.88 ± 0.19 eV
	Linear segments (y= mx+b)	Linear segments (y= mx+b)
(b)	Base line: 2.5512 × 10^{-1} ≤ hν ≤ 2.4311 eV	Base line: 2.2061 ≤ hν ≤ 2.4406 eV
(c)	m= 2.5512 × 10^{-1} ± 4.8196 × 10^{-3}	m= 8.6716 × 10^{-2} ± 5.0100 × 10^{-3}
(d)	b= 1.8463 × 10^{-2} ± 1.1223 × 10^{-2}	b= 3.5505 × 10^{-2} ± 1.1626 × 10^{-2}
(e)	r-square= 0.992	r-square= 0.920
(f)	Tauc: 3.2974 eV ≤ hν ≤ 3.5834 eV	Tauc: 3.2287 eV ≤ hν ≤ 3.5223 eV
(g)	m= 1.117 ± 2.1701 × 10^{-2}	m= 6.3071 × 10^{-1} ± 1.1945 × 10^{-2}
(h)	b= -2.4089 ± 7.4603 × 10^{-2}	b= -1.5316 ± 4.0287 × 10^{-2}
(i)	R-square= 0.995	R-square= 0.995
	Attributes description	
(a)	Number and band gap energy (*Eg*) value*	
(b)	hν- range of the base line segment	
(c)	Slope and standard error of the base line segment	
(d)	Intercept and standard error of the base line segment	
(e)	R^2 of the straight-line fit of the base line segment	
(f)	hν- range of the Tauc segment	
(g)	Slope and standard error of the Tauc segment	
(h)	Intercept and standard error of the Tauc segment	
(i)	R^2 of the straight-line fit of the Tauc segment	

* The error of the band gap energy is calculated from the standard errors of the Tauc and Base straight-line equations. In practice, this error could be interpreted as the estimation of the dispersion of the band gap energy determined by manual methods [3].

an autoclave with a nitrogen solution of urea (99.9% Fisher Scientific) in deionized water (0.0178 M), in order to introduce the required molar amount of nitrogen (2.5 wt% to the precursor). Finally, a thermal treatment step was performed to promote the crystallization of TiO_2-N NPs with a heating rate of 7 °C/min until reaching 200 °C, after which was sustained for 6 h.

Following the thermal treatment step, the synthesised NPs were washed with deionized water, centrifuged, and dried at room temperature to obtain the nitrogen doped TiO_2 nanopowder (TiO_2-N).

Fig. 11 summarises the methodology used to synthesise the nitrogen-doped TiO_2 nanoparticles, as well as all previously reported TiO_2-based NPs [1] for which additional characterization data are provided in this data in brief.

Photocatalytic data- UV-Vis profiles

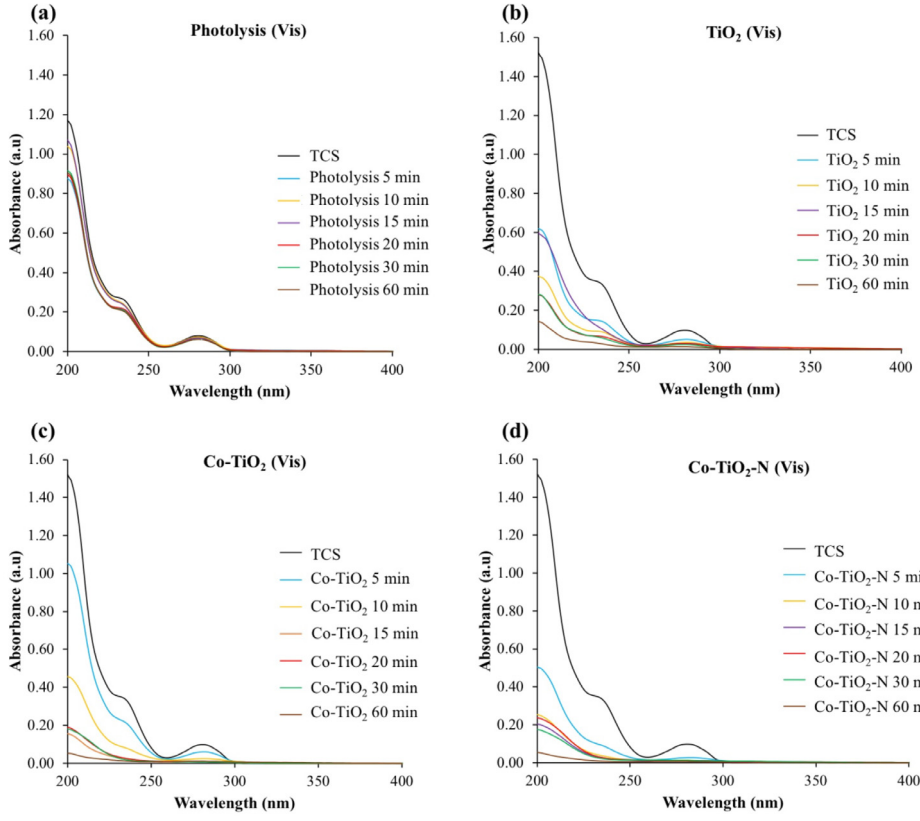

Fig. 5. UV-Vis spectra of the post-reaction solutions of triclosan (TCS) degradation in the (a) absence (photolysis) and (b) presence of TiO_2, (c) cobalt doped TiO_2 (Co-TiO_2) and (d) cobalt and nitrogen co-doped TiO_2 (Co-TiO_2-N) nanocatalysts, under Vis (450 nm) light exposure conditions for 5, 10, 15, 20, 30 and 60-minutes.

2.2. Photocatalytic LED-reaction system

Photocatalytic reaction tests to evaluate the photoactivity of nanocatalysts were performed in a Penn *PhD* photoreactor M2 as previously reported [1]. The catalytic reactions took place in 40 mL borosilicate vials containing 10 mL of an aqueous TCS solution (10 ppm) to which the nanocatalysts were added and dispersed (1 g/L). The dispersions were further exposed to monochromatic irradiation (λ = 450 nm) provided by a blue LED lamp (3.4 W at 100% light intensity) for periods of 60 min, under continuous magnetic stirring (900 rpm) and controlled temperature (SP = 35 °C) regulated by a fan and a coupled J-type thermocouple (simplex, IEC60584, ΔT = - 40 a 350 °C).

The post-reaction TCS solutions were further analysed by UV-Vis spectrometry and High-performance liquid chromatography (HPLC).

High-performance liquid chromatography (HPLC) data- Chromatograms and TCS calibration curve

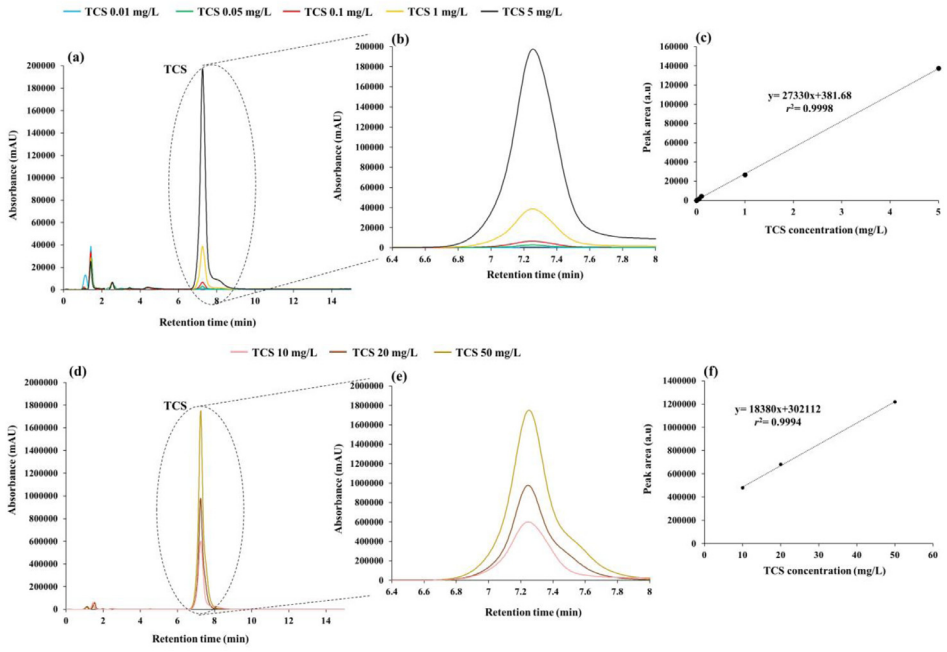

Fig. 6. Chromatograms of triclosan (TCS) standard solutions at (a) lower and (b) higher concentrations ranges for calibration purposes; (b) and (c) correspond to amplified ranges including the main characteristic TCS band; and (c) and (f) are the fitted data to the linear regression model of each TCS concentration range.

2.3. Brunauer-Emmett-teller (BET) analysis

Nitrogen (N_2) adsorption/desorption isotherms at low temperature (-196 °C) were acquired in an automatic Quantachrome NOVA 2200e equipment, and further used to determine the apparent surface areas ($A_{B.E.T.}$) of TiO_2-based NPs using the B.E.T model [6] as previously described [1].

2.4. X-ray photoelectron spectroscopy (XPS)

The atomic elemental composition as well as metals oxidation states at the synthesised NPs surfaces were determined by XPS in a dual anode KRATOS XSAM800 spectrometer with Vision 2 for Windows, Version 2.2.9 from KRATOS for data acquisition. The samples (powders) were mounted on the sample holder through a double-side tape. The analyses were performed with a non-monochromatic AlKα X-ray source (1486.7 eV), produced with a current of 10 mA and an anode voltage of 12 kV, operating at Fixed Analyzer Transmission (FAT) mode, with a pass energy of 20 eV. Samples were analysed using 90° and 30° take-off angles (relative to the surface plane) in an ultrahigh vacuum chamber ($\sim 10^{-7}$ Pa) at room temperature. The sensitivity factors used for quantification analysis were: 0.28 C 1s; 0.78 for O 1s; 2.00 for Ti 2p; 2.40 for Co $2p_{3/2}$ and 0.48 for N 1s. The effect of the electric charge accumulation was corrected using as reference the carbon peak (set at 285 eV), assigned to sp^3 carbon atoms bonded to carbon and/or hydrogen.

High-performance liquid chromatography (HPLC) data- Chromatograms of TCS post-reaction solutions

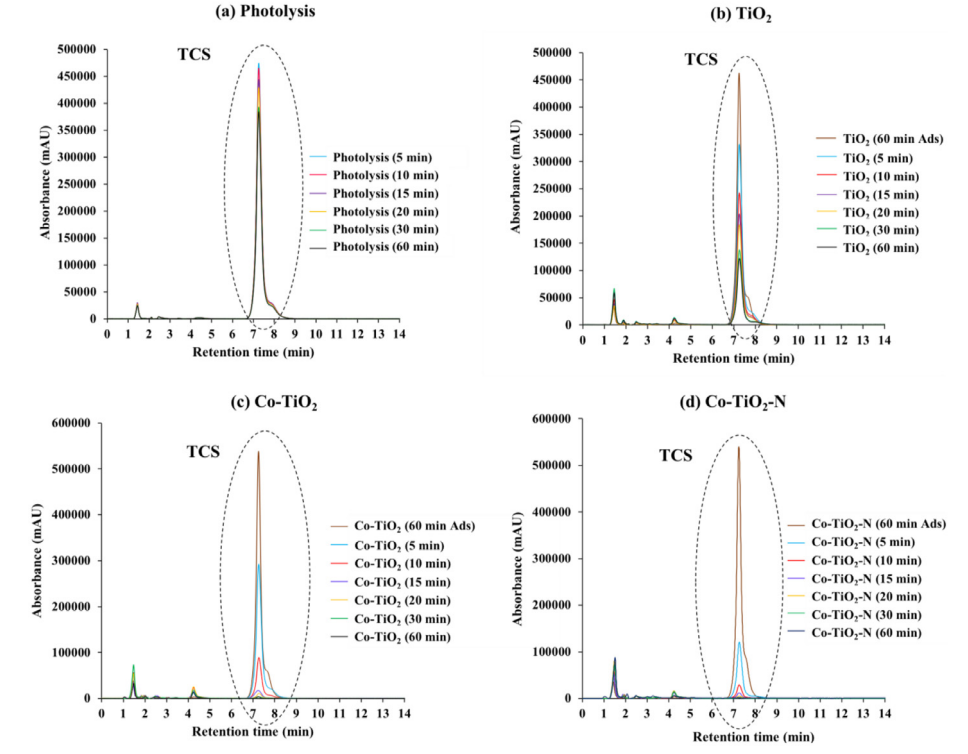

Fig. 7. HPLC chromatograms of TCS post-reaction solutions in the (a) absence (photolysis) and (b) presence of TiO_2, (c) cobalt doped TiO_2 (Co-TiO_2) and (d) cobalt and nitrogen co-doped TiO_2 (Co-TiO_2-N) nanocatalysts for 60 minutes under dark (only in the presence of nanoparticles), and after 5, 10, 15, 20, 30 and 60-minutes under visible (450 nm) LED light exposure conditions.

2.5. Diffuse reflectance spectroscopy (DRS)

The optical properties of the TiO_2-based NPs were obtained on a UV-Vis spectrometer Shimadzu UV-2600 PC equipped with an ISR 2600 plus integrating sphere, as described in [1], using barium sulphate ($BaSO_4$) as reference. The bandgap energy (*Eg*) of the synthesised samples were determined from diffuse reflectance spectra using the GapExtractor v1.0 automated method. This method is based on a five-step algorithm that simulates an expert analyst's judgment in identifying linear segments in plots and estimating the *Eg* value. Before data acquisition, a baseline correction was performed with $BaSO_4$.

2.6. UV-Vis spectroscopy (UV-Vis)

UV-Vis spectra were collected at wavelengths ranging from 200 to 400 nm by using a Shimadzu UV-1900 UV-Vis spectrophotometer. For data acquisition, a bandwidth of 1 nm (average response) and a scanning speed of 400 nm/min were used, and a baseline correction with the solvent used to prepare TCS solutions was also performed before data acquisition.

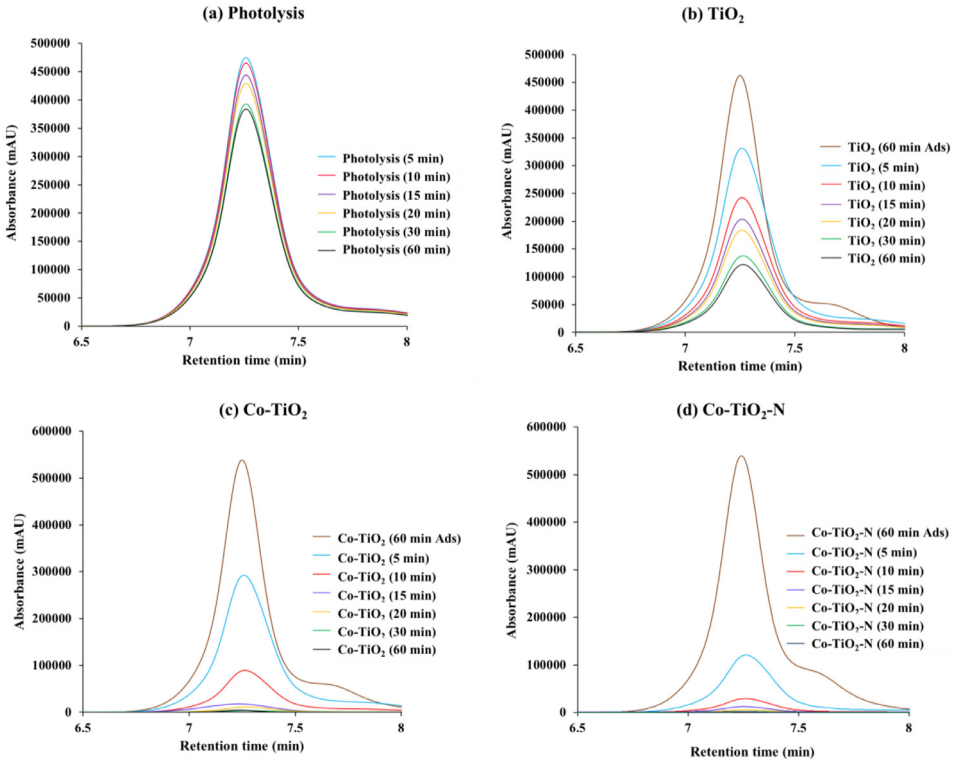

Fig. 8. HPLC chromatograms of TCS post-reaction solutions in the (a) absence (photolysis) and (b) presence of TiO_2, (c) cobalt doped TiO_2 (Co-TiO_2) and (d) cobalt and nitrogen co-doped TiO_2 (Co-TiO_2-N) nanocatalysts for 60 minutes under dark (only in the presence of nanoparticles), and after 5, 10, 15, 20, 30 and 60-minutes under visible (450 nm) LED light exposure conditions.

2.7. High-performance liquid chromatography (HPLC)

HPLC chromatograms of TCS solutions were obtained as described in detail in our previous work [1]. In addition, a prior to the HPLC analysis, the TCS post-reaction solutions were filtered using a syringe-filter (0.22 µm, TPP, Switzerland) to remove the NPs. TCS solutions standards of known concentrations (0.01, 0.05, 1 and 5 ppm) were prepared and used for calibration purposes.

2.8. X-ray powder diffraction (XRD)

For the X-ray powder diffraction (XRD) patterns acquisition, the TiO_2-based NPs were prior mounted on a silicon amorphous sample holder, and further acquired in a Philips Analytical, PW 3050/60 with automatic data acquisition supported by the X'Pert Data Collector v.2.0b software and employing a CuKα radiation ($\lambda = 0.15406$ nm) working at 40 kV/30 mA, following a data collection methodology as prior described [1].

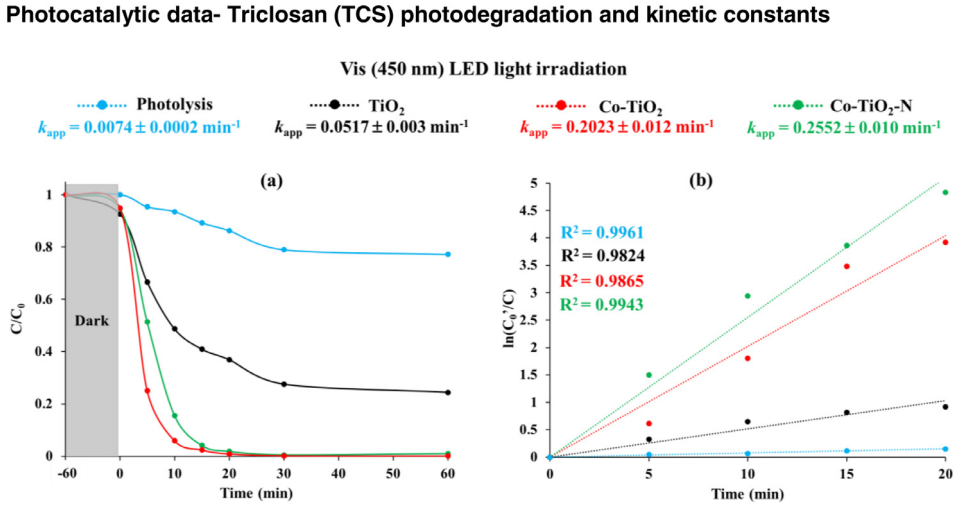

Fig. 9. Photocatalytic degradation of TCS aqueous solutions (≅ 10 ppm) during 60 min under exposure to Vis LED light (λ = 450 nm) in the presence and absence (photolysis) of the synthesised TiO_2, TiO_2 doped with cobalt (Co-TiO_2) and TiO_2 co-doped with cobalt and nitrogen (Co-TiO_2-N) nanocatalysts (a); and the corresponding kinetics of the photocatalytic degradation of TCS, following a pseudo-first order kinetic model, including the respective obtained coefficients (R^2) and apparent first-order rate constants (k_{app}) (b).

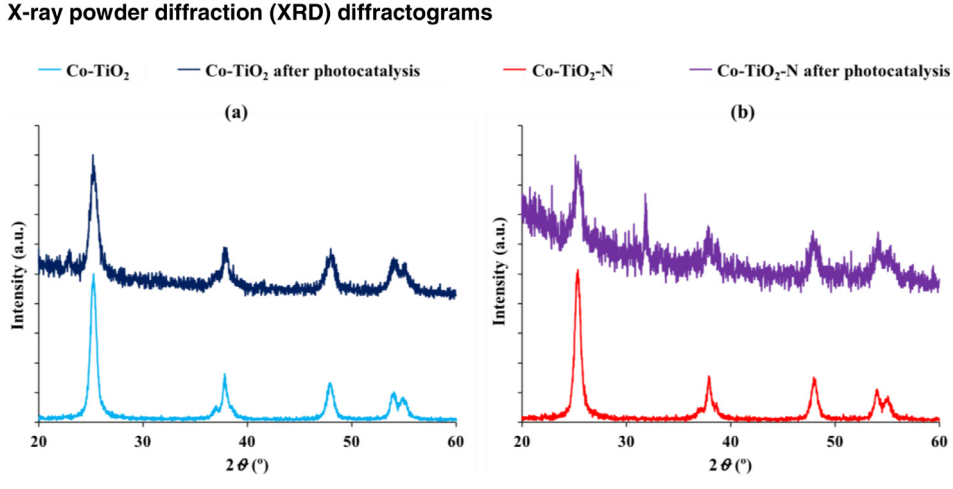

Fig. 10. XRD diffractograms obtained for (a) TiO_2 doped with cobalt Co-TiO_2 and (b) TiO_2 co-doped with cobalt and nitrogen (Co-TiO_2-N) before and after four photocatalytic successive runs of TCS degradation reactions.

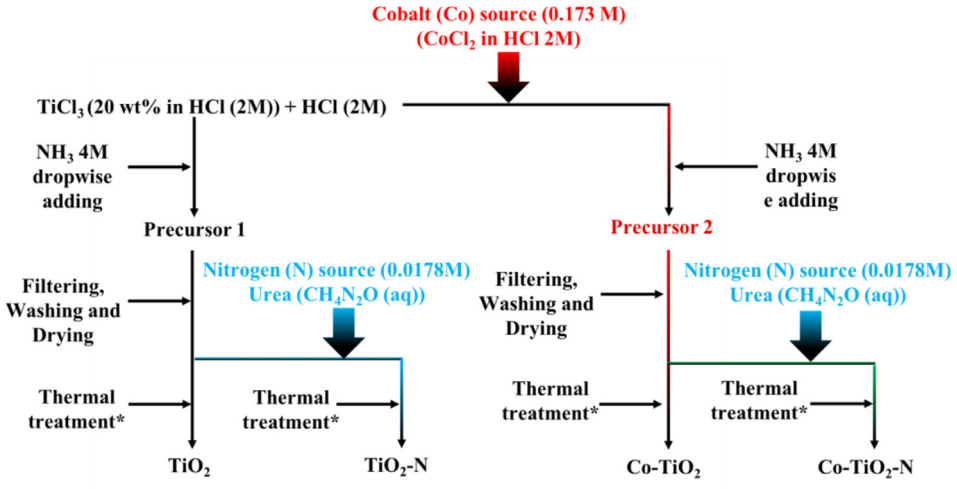

Fig. 11. Methodology of synthesis and doping with cobalt (Co) and nitrogen (N) of TiO_2 nanoparticles.

Declaration of Competing Interest

The authors declare that they have no known competing financial interests or personal relationships that could have appeared to influence the work reported in this paper.

CRediT Author Statement

Olga Ferreira: Formal analysis, Investigation, Data curation, Writing – original draft; **Olinda C. Monteiro:** Resources; **Ana M. Botelho do Rego:** Resources, Data curation, Writing – review & editing; **Ana M. Ferraria:** Formal analysis, Writing – review & editing; **Mary Batista:** Formal analysis; **Elisabete R. Silva:** Conceptualization, Methodology, Investigation, Resources, Data curation, Writing – review & editing, Supervision.

Acknowledgments

This research work was supported by national funds through FCT-Foundation for Science and Technology within the scope of research units grants to BioISI (UIDB/04046/2020 and UIDP/04046/2020) and CQE (UIDB/00100/2020) and iBB (UIDB/04565/2020 and UIDP/04565/2020) and i4HB (LA/P/0140/2020).

O. Ferreira also acknowledges the Grant PD/BD/128370/2017 through FCT. E.R. Silva and M. Batista and A.M. Ferraria thank FCT for the work contract through the Scientific Employment Stimulus-Individual Call (CEECIND/03530/2018) and Investigators contracts-DL57, respectively.

Supplementary Materials

Supplementary material associated with this article can be found in the online version at doi:10.1016/j.dib.2021.107696.

References

[1] O. Ferreira, O.C. Monteiro, A.M. Botelho do Rego, A.M. Ferraria, M. Batista, R. Santos, S. Monteiro, M. Freire, E.R. Silva, Visible light-driven photodegradation of triclosan and antimicrobial activity against Legionella pneumophila with cobalt and nitrogen co-doped TiO_2 *anatase* nanoparticles, J. Environ. Chem. Eng. 9 (6) (2021) 106735, doi:10.1016/j.jece.2021.106735.

[2] A. Escobedo-Morales, I.I. Ruiz-López, M.deL. Ruiz-Peralta, L. Tepech-Carrillo, M. Sánchez-Cantú, J.E. Moreno-Orea, Automated method for the determination of the band gap energy of pure and mixed powder samples using diffuse reflectance spectroscopy, Heliyon 5 (4) (2019) e01505, doi:10.1016/j.heliyon.2019.e01505.

[3] A. Escobedo-Morales, I.I. Ruiz-López, GapExtractor © version 1.0. User's Guide, 2018.

[4] M.R. Nunes, O.C. Monteiro, A.L. Castro, D.A. Vasconcelos, A.J. Silvestre, A new chemical route to synthesise TM-doped (TM = Co, Fe) TiO_2 nanoparticles, Eur. J. Inorg. Chem. 6 (2008) 961–965, doi:10.1002/ejic.200700978.

[5] B. Barrocas, O.C. Monteiro, M.R. Nunes, A.J. Silvestre, Influence of Re and Ru doping on the structural, optical and photocatalytic properties of nanocrystalline TiO_2, SN Appl. Sci. 556 (2019) 1–12 1, doi:10.1007/s42452-019-0567-4.

[6] M. Thomees, K. Kaneko, A.V. Neimark, J.P. Olivier, F. Rodriguez-Reinoso, J. Rouquerol, K.S.W. Sing, Physisorption of gases, with special reference to the evaluation of surface area and pore size distribution (IUPAC technical report), Pure Appl. Chem. 87 (2015) 1051–1069 19511069, doi:10.1515/pac-2014-1117.